Design and Simulation of High Frequency Inverter for PV System

R. Ramalingam
ME Scholar; Dept. of EE,
Govt College of Technology,
Coimbatore, india,

Dr. P. Maruthupandi,
Assistant Professor,
Dept. of EEE,
Govt College of Technology,
Coimbatore, india,

S. Karthick
ME Scholar; Dept. of EE,
Govt College of Technology,
Coimbatore, india,

Abstract— **In this paper, a high frequency a link photovoltaic (PV) inverter. The proposed inverter most of the problem associated with currently available photovoltaic (PV) inverter, A single stage power conversion unit is found to fulfill all the system requirements like inverting dc voltage to ac voltage, step up or step down the input voltage, (MPPT) generating low harmonics at the output voltage, and input/output isolation. This partial resonant ac link converter in which the link is formed by a partial inductor/capacitor (LC) pair. The significant merits of the proposed inverter are the zero voltage turn on and soft turn off of the switches which results in reduce the switching losses an minimum stress on the switches. For Any fault on the grid side is compensated by the reactive power injection from the universal bridge to maintain the constant output voltage. The simulation of the proposed high frequency inverter is carried out and results are analysed.**

Index Terms—Inverters, photovoltaic (PV) systems, zero-voltage switching (ZVS).

I.   INTRODUCTION

Power electronics is an integral part of these distributed energy systems as they convert generated electricity into utility compatible form. However, the additional of power electronics usually add costs as well as certain reliability issues [1], [2].

Referring to a report by Sandia National Laboratories (SNL) [3], inverters are responsible for most of the photovoltaic PV system incidents trigger in the field. They are cost and complex, and their current mean time to first failure is unacceptable. Inverter failure contribute to unreliable photovoltaic (PV) system, which may result in loss of confidence in renewable technology. Therefore, to achieve long-term success in the photovoltaic (PV) industry, new power converters with high reliability and long life time are required [3], [4].

In past design, a centralized converter-based photovoltaic (PV) system was the most commonly used type of photovoltaic (PV) system. For voltage source inverter (VSI)

connected to the photovoltaic (PV) modules. The inverter output of each phase is connected to an LC filter to limit the harmonic. A three phase transformer, which step up the voltage connect the inverter to the utility [1].
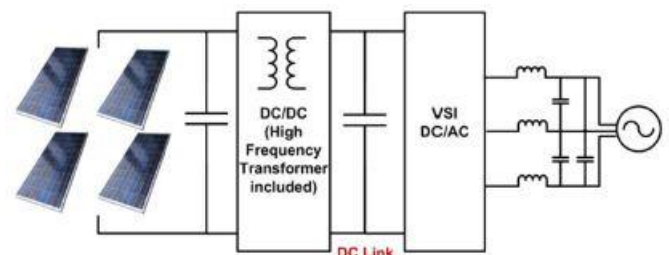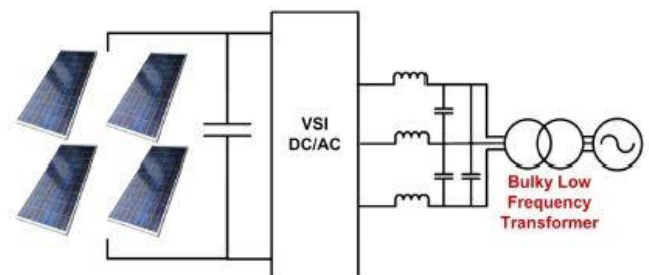

Fig.1.Converter -Based PV System

Fig.2.Multi-Stage Conversion System

Low frequency transformer are considered poor components mainly due to large size and produce low efficiency. So to avoid low frequency transformer, multiple stage conversion system are widely used in photovoltaic (PV) systems [5], [6]. The most common topology dc–ac voltage source inverter (VSI) and a dc–dc converter. Commonly, the dc–dc converter contains a high frequency transformer [1]. this converter consists of multiple power processing stages which produce the low efficiency of the overall system. Moreover, bulky electrolytic capacitors are required for the dc link. Electrolytic capacitors, which are very sensitive to temperature, may cause severe reliability problems for inverters, and an increase of even 10∘C can halve their lifetime [7]. Therefore, PV inverters containing electrolytic capacitors are not expected to provide the same lifetime as PV modules.

Consequently, the actual cost of the PV system involves the periodic replacement of the inverter, which increases the levelized cost of energy extracted from the PV system [8].
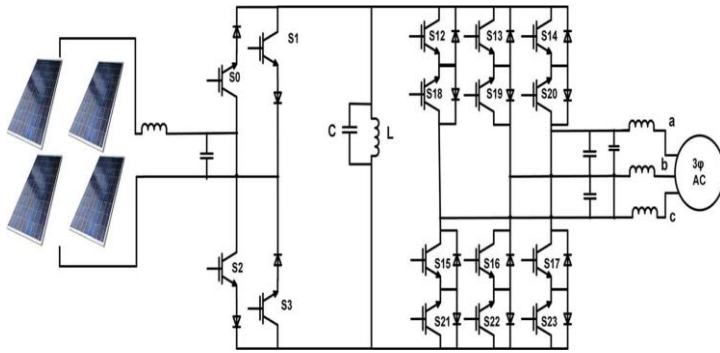

Fig.3. Proposed inverter

Consider the aforementioned problems, it is essential to support the design of alternative inverter topologies to reduce the cost of the inverter while increase reliability [7]. Several solutions have been proposed to partially overcome these problems. Reference [5] introduces a transformerless topology in which the ground leakage current is minimized; however, the voltage cannot change over a wide range. Reference [9] proposes an integrated solution for a PV/FC based hybrid distributed generation system to eliminate the requirement of high-voltage buffer capacitors for inverters. This type of inverter, nonetheless, does not provide isolation. In [10], large electrolytic capacitors are replaced by small film capacitors; however, the proposed solution is merely applicable in low power PV systems.

A number of resonant PV inverters have been proposed as well [11], [12]. A high frequency link photovoltaic (PV) power conditioning system which includes a high frequency resonant inverter, a rectifier, and a line commutated inverter, operating near unity power factor, has been proposed in [11]. Three other resonant photovoltaic (PV) inverter are introduced in [12]: high frequency resonant inverter cyclo converter, high frequency resonant inverter rectifier pulse width modulated (PWM) voltage source inverter(VSI), and high frequency resonant inverter rectifier line connected inverter. All of these resonant PV inverter contain multiple stages. The first and fourth inverters require a large inductor for dc current link, and the third configuration needs a large dc link capacitor.

A high frequency ac link PV inverter which overcomes most of the problems associated with existing inverters is proposed in this paper. The proposed inverter is a partial resonating converter, only a small time interval is allocated to resonance in each cycle. Hence, while the resonance facilitates the zero-voltage turn-on of the switches, the inductor/capacitor (LC) link has low reactive ratings and low power dissipation. Due to the soft switching, very high switching losses in this inverter are negligible and the frequency of the link., resulting in a compact link inductor. Moreover, the zero voltage turn on results in switches on the voltage stress can be reduce.

The merit of the proposed inverter is the elimination of the dc link and the replacement of the bulky electrolytic capacitors employed in the multiple stage conversion systems with an inductor/capacitor (LC) pair having alternating current and voltage. The present authors have introduced the partial resonant PV inverter in [13].

II. PROPOSED INVERTER AND PRINCIPLE OF OPERATION

Fig. 3 represent the proposed photovoltaic (PV) inverter. Four unidirectional switches forming the PV switch bridge interface the PV modules to the link, and six bidirectional switches forming the ac side switch bridge connect the same link to the load. Since PV cells cannot absorb electrical energy, the associated switch bridge is formed merely by unidirectional switches. Any fault on the grid side is compensated by reactive power injection from a universal bridge to maintain the output voltage constant.

This inverter is, in essence, a dc to ac buck boost converter in which the link is charged through the PV and then discharged into the output phases. The charging and discharging take place alternative. The frequency of charge/discharge is called the output line frequency higher than the link frequency.
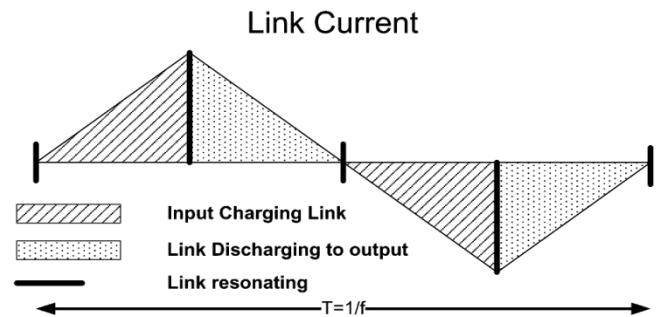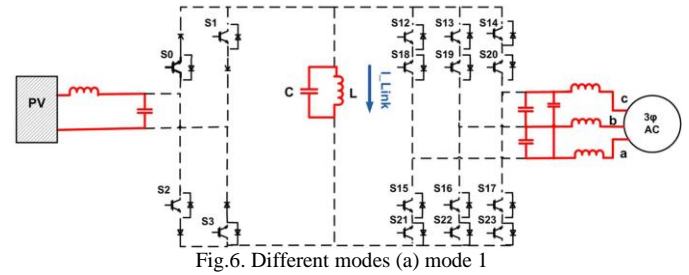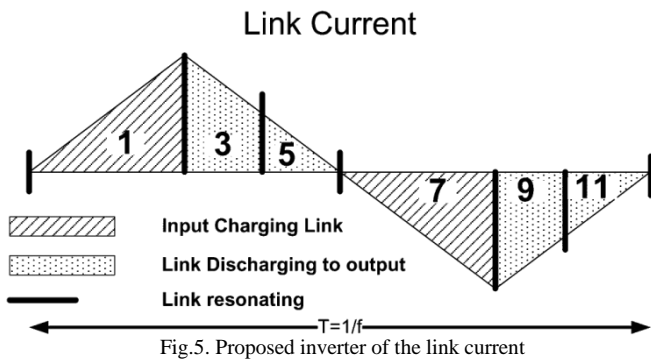

Fig.4. Ac link buck boost converter

Switches on each leg facilitate the charging and discharging of the link in a reverse direction, leading to an alternative current in the link. The alternating current of the link results in better utilization of the inductor/capacitor (LC). Figure. 4 depicts the link current in a ac link buck boost inverter. As represented in this figure, between each charging and discharge, there is a resonant mode during which none of the switch conduct and the inductor/capacitor (LC) link resonates to facilitate the zero voltage turn on of the switches. The general control strategy is to turn on each switch such that its turn-on occurs at zero voltage and to turn off the switches when the input or output currents meet their references. The negligible switching losses of this inverter allows the use of slower switches with higher current density, possibly with soft-switched optimized structures or, alternatively, higher link frequency. A dc to dc buck boost converter, the input and output of this inverter appear as voltage sources. Therefore, filter capacitors are placed across the input and output terminals as represented in Fig. 3.

Special Issue - 2015

International Journal of Engineering Research & Technology (IJERT)
ISSN: 2278-0181
TITCON-2015 Conference Proceedings

Fig.5. Proposed inverter of the link current

The basic operating modes and relevant waveforms of this inverter are represented in Figs. 6, respectively. The link mode of operation is divided into 12 modes, with six power transfer modes and six resonating modes. The link is energized from the input during modes 1 & 7 and is de-energized to the output during modes 3, 5, 9, & 11. Modes 2, 4, 6, 8, 10, & 12 are devoted to resonance.
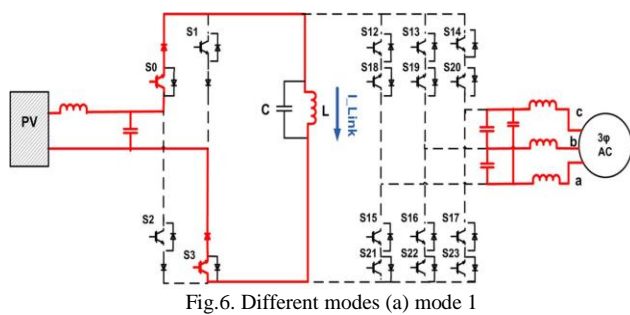
III.   MODES OF OPERATION

A detail description of the modes of operation is follows.

Mode 1 (Energizing): The start of mode 1, proper switches on the photovoltaic (PV) switch bridge, for switch conduct during mode 1, are activated S0 and S3 turn on in . 6 ; however, they do not immediately conduct since they are reverse biased. The link voltage which is resonant before mode 1, becomes equal to the photovoltaic (PV) voltage, the proper switches S0 and S3 are forward biased. This results in the zero voltage turn on of S0 and S3.. The link current (i_{Link}) during mode 1 an be calculated using the following: In (1) and (2), L and V_{PV} are the link inductance and PV voltage, respectively. During this mode the link voltage is equal to V_{PV}.

Fig.6. Different modes (a) mode 1

The link is charged until the PV current, average over a cycle time, meet it reference value. The switches located on the PV switch bridge are then turned off. As mentioned earlier, the link capacitor acts as a buffer across the switches during their turn-off, which results in low turn-off losses.

(Partial resonance): During mode 2, none of the switches conduct and the link resonates, link voltage value can be decrease. The following equation describes the behavior of the *LC* circuit ($i_c(t)$, $V_{Link(t)}$, and *C* are the capacitor current, link voltage, and link capacitance.

Fig.6. Different modes (a) mode 1

The current flow through the capacitor is equal to "$-i_{Link}(t)$" and the inductor (L) current is positive (+Ve), resulting in negative (-Ve) $dV_{Link(t)}/dt$. This implies that the link voltage value is decreasing. Once the link voltage becomes negative (-Ve), the controller determines which output phase pairs have to be charged on the link during modes 3 and 5. The sum of the output reference current can be instant is zero. One of them is the high in magnitude and of certain polarity while the two lower ones are of the opposite polarity. Although there are three phase pairs in a three phase system, considering the polarity of the current in each phase, only two of these phase pairs can provide a path of current when connected to the link.

Therefore, the charged link transfers power to the output by discharging into two phase pairs. The two phase pairs are the one formed by the phase having the highest and second highest reference currents and the one formed by the phase having the highest and lowest reference currents, where the reference currents are sort as highest, second high, and low in term of magnitude alone. For example, if $I_{a\_o} = -10$ A, $I_{b\_o} = 7$ A, and $I_{c\_o} = 3$ are the three output reference current, then phase pairs ab & ac are chosen to transfer power to the output. The phase pair with smaller line-to-line voltage is the first one the link is discharged to. For examples, if $V_{ab\_o} = 300$ V and $V_{ac\_o} = 400$ V, the link will be first discharged into phase pair ab.
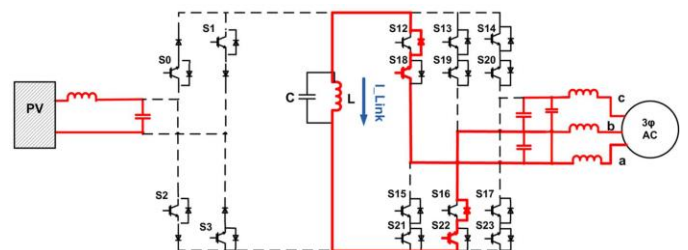
Mode 3 (De-energizing): The output switches S18 and S22) are turned on at zero voltage to allow the link to be discharged into the chosen phase pair until the current of phase b at the output side averaged over a cycle time meet its reference. At this point, switches S22 can turn off, initiating another resonating mode.

(c) Mode 3.

Mode 4 (Partial resonance): The link is allow to swing to the   voltage of the   other output phase pair chosen during mode 2. For the case shown in Figs. 6, the link voltage swings from V_{ab-o} to V_{ac-o}.

Mode 5 (De-energizing): During mode 5, the link discharge to the selected output phase pair until there is just

Special Issue - 2015

International Journal of Engineering Research & Technology (IJERT)
ISSN: 2278-0181
TITCON-2015 Conference Proceedings

sufficient energy left in the link to swing to a predetermined voltage (V_{max}), higher than the maximum input and output line-to-line voltage. At the end of mode 5, for all the switch can be turned off condition, allowing the link to resonate during mode 6.

(d) Mode 5.

Mode 6 (Partial resonance): During mode 6, the link voltage swings to V_{max}, and then, its absolute value decreases. Proper switches, which are supposed to conduct during mode 7, are turned on during this mode; however, they do not conduct as they are reversed biased.

Modes 7 to 12 are similar to mode 1 to 6, except that the link charge and discharge in the reverse direction. the compliment switch on each leg is switched when compared with the ones switched during mode 1 to 6. As seen in Fig. 6, the input- and output-side switches never conduct simultaneously, which implies that the input and output are isolated. A single-phase high frequency transformer can be added to the link. In this case, the magnetizing inductance of the transformer can play the role of the link inductance.

IV. SIMULATION AND RESULTS

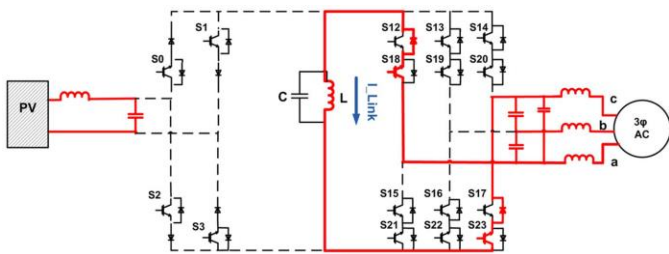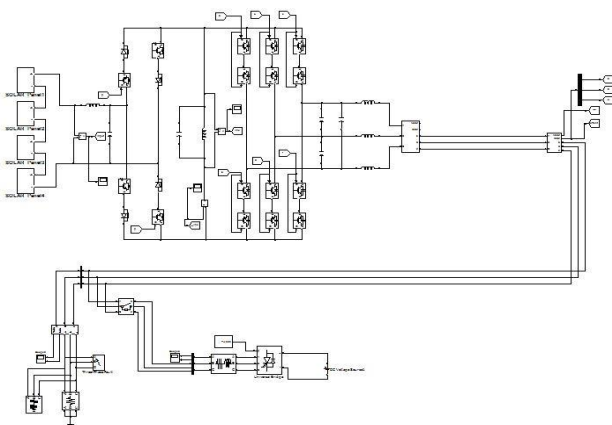A 30-kW PV inverter has been designed, and the parameters are summarized in Table I.

Fig.7 Simulation Of Proposed Inverter

The link capacitance in the prototype is 0.8 μF, which is much higher than the amount achieved through the design procedure. Although the resonating time is preferred to be as short as possible, it should be long enough to allow microcontroller or processor to turn on the proper switches prior to the next energizing or de energizing mode. Due to the

processor limitation, the link capacitance has been chosen as

0.8 μF in the prototype. The designed PV inverter has been simulated in MATLAB, and Fig. 8 represent the simulation results. In Fig. 9, the link capacitance 0.8 μF value.

TABLE 1

SIMULATION PARAMETERS

Parameter	Value
Nominal PV Voltage	700 V
Output Voltage	480 V (rms, line to line)
Link Inductance	110 μH
Link Capacitance	Prototype: 0.8 μF Simulation: 0.8 μF and 0.1 μF
Peak of Link Current	200 A with 0.8 μF link capacitance 180 A with less than 0.1 μF link capacitance
Link frequency	7.2 kHz with 0.8 μF link capacitance 8.5 kHz with less than 0.1 μF link capacitance
PV side filter	Inductance: 200 μH Capacitance: 150 μF
ac side filter	Inductance: 50 μH Capacitance: 72 μF (line to line)

Fig. 8 represent the input voltage full power. The input voltage is 700 V, and the input current is 43 A. In this case, the power factor is close to unity and the frequency is 50 Hz.
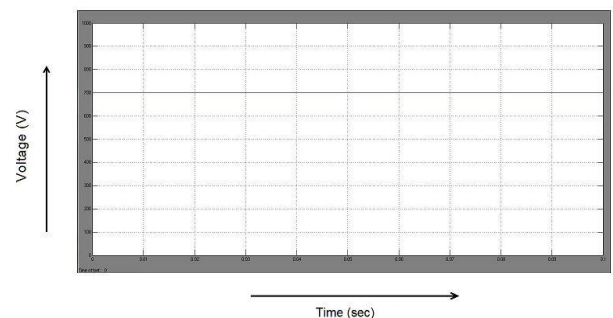

Fig.8 Photovoltaic (PV) Input Voltage Waveform.

Fig. 9 represent the link current, respectively. The link current and voltage are both alternating. Since the frequency of the link (7200 Hz) is much higher than the frequency of the line (50 Hz), the link voltage and current are illustrated in these figure over a short time interval. As it can be seen in these figures that the predetermined voltage to which the link resonates during mode 6 is set at 850 V. Moreover, the peak of the link current is 200 A, although during mode 1, the link current is increase to 180 A. During mode 2, as the link resonate, its peak current reach 200 A. As previously mentioned, the higher the link capacitance is, the longer the resonating time will be. Fig. 9 depicts the link current at full power using 0.1-μF link capacitance. As seen in this figure, the peak of the link current in this case is very close to the calculated value [using (10)] which is 180 A.

Special Issue - 2015

International Journal of Engineering Research & Technology (IJERT)
ISSN: 2278-0181
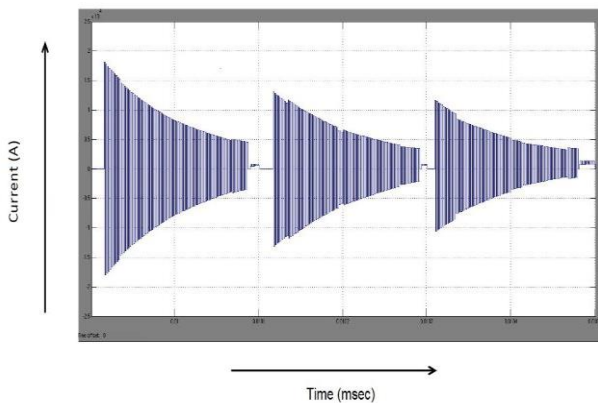**TITCON-2015 Conference Proceedings**

Fig.9 Simulation Of Link Current

At lower power level, the peak of the link current will be lower than that of the full power. Fig. 9 represent the link current at 15 kW. As seen in this figure, the predetermined voltage to which the link resonates during mode 6 is still set at 850 V. Although the PV voltage has dropped to 350 V, the maximum output line-to-line voltage is still 679 V. The peak of the link current in this case is about 147 A. Again, the resonating time is noticeable due to the use of 0.8-μF link capacitance.
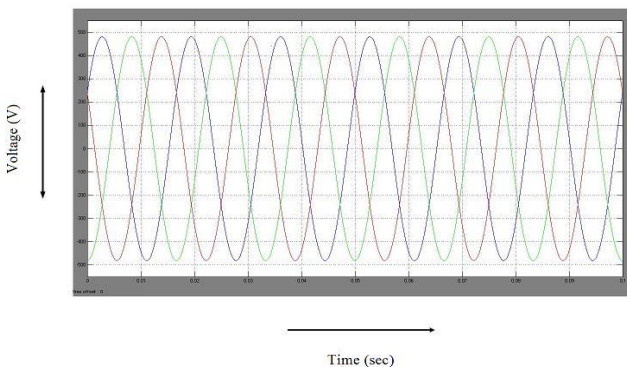

Fig.10 Ac Output Voltage Waveform

The simualtion model of the system with high frequency inverter is shown in figure 10. Any fault on the grid side is compensated by reactive power injection from a universal bridge to maintain the output voltage constant. The simulation model of the system with high frequency inverter are implemented in MATLAB and the simulation is carried out.

V. CONCLUSION

In this paper, a reliable and compact PV inverter has been proposed. This inverter is a partial resonant ac-link converter in which the link is formed by an inductor/capacitor (LC) pair having alternating current and voltage. The proposed converter guarantees the isolation of the input and output. The link inductance can be replaced by a single-phase high frequency transformer. The elimination of the dc link and low frequency transformer makes the proposed inverter more compact and reliable compared with other types of

photovoltaic (PV) inverter. In this paper, the principle of operation of the proposed converter along with the detailed design procedure has been presented. Any fault on the grid side is compensated by reactive power injection from a universal bridge to maintain the output voltage constant. The performance of the proposed converter has been evaluated through both simulation results.

REFERENCES

[1] S. Chakraborty, B. Kramer, and B. Kroposki, "A review of power electronics interfaces for distributed energy systems towards achieving low-cost modular design", *Renew. Sustain. Energy Rev.*, vol. 13, no. 9, pp. 2323–2335, Dec. 2009.

[2] Y. Huang, F. Z. Peng, J. Wang, and D. W. Yoo, "Survey of the power conditioning system for PV power generation", in *Proc. IEEE PESC*, Jun. 18–22, pp. 1–6, 2006.

[3] S. Atcitty, J. E. Granata, M. A. Quinta, and C. A. Tasca, Utility-scale gridtied PV inverter reliability workshop summary report, Sandia National Labs., Albuquerque, NM, USA SANDIA Rep. SAND2011-4778.

[4] Y. C. Qin, N. Mohan, R. West, and R. Bonn, Status and needs of power electronics for photovoltaic inverters, Sandia National Labs., Albuquerque, NM, USA, SANDIA Rep. SAND2002-1535.

[5] T. Kerekes, R. Teodorescu, P. Rodríguez, G. Vázquez, and E. Aldabas, "A new high-efficiency single-phase transformerless PV inverter topology", *IEEE Trans. Ind. Electron.*, vol. 58, no. 1, pp. 184–191, Jan. 2011.

[6] G. Grandi, C. Rossi, D. Ostojic, and D. Casadei, "A new multilevel conversion structure for grid-connected PV applications", *IEEE Trans. Ind. Electron.*, vol. 56, no. 11, pp. 4416–4426,

[7] R. Margolis, A review of PV inverter technology cost and performance projections, Nat. Renew. Energy Lab., Golden, CO, USA, NREL/SR-620- 38771, Nov. 2009.

[8] S. J. Castillo, R. S. Balog, and P. Enjeti, "Predicting capacitor reliability in a module-integrated photovoltaic inverter using stress factors from an environmental usage model". in *Proc. NAPS*, pp. 1–6, 2010.

[9] S. Jain and V. Agarwal, "An integrated hybrid power supply for distributed generation applications fed by nonconventional energy sources". *IEEE Tran. Energy Convers.*, vol. 23, no. 2, pp. 622–63, Jun. 2008.

[10] C. Rodriguez and G. A. J. Amaratunga, "Long-lifetime power inverter for photovoltaic AC modules". *IEEE Trans. Ind. Electron.*, vol. 55, no. 7, pp. 2593–2601, Jul. 2008.

[11] A. K. S. Bhat and S. B. Dewan, "A novel utility interfaced high-frequency link photovoltaic power conditioning system", *IEEE Trans. Ind. Electron.*, vol. 35, no. 1, pp. 153–159, Feb.1988.

[12] A. K. S. Bhat and S. B. Dewan, "Resonant inverters for photovoltaic array to utility interface", *IEEE Trans. Aerosp. Electron. Syst.*, vol. 24, no. 4, pp. 377–386, Jul.1988.

[13] M. Amirabadi, A. Balakrishnan, H. A. Toliyat, and W. Alexander, "Soft switchedAC-link direct-connect photovoltaic inverter", in *Proc. IEEE Int. Conf. Sustain. Energy Technol.*, pp. 116–120, 2008.

[14] A. Balakrishnan, H. A. Toliyat, and W. C. Alexander, "Soft switched AC link buck boost converter", in *Proc. IEEE APEC*, pp. 1334–1339, 2008.

[15] A. Balakrishnan, M. Amirabadi, H. Toliyat, and W. Alexander, "Soft switched AC link wind power converter", in *Proc. IEEE ICSET*, pp. 318–321, 2008.

[16] M. Amirabadi, H. A. Toliyat, and W. C. Alexander, "Battery-utility interface using soft switched AC link buck–boost converter", in *Proc. IEMDC*, pp. 1299–1304, 2009.

[17] M. Amirabadi, H. A. Toliyat, and W. C. Alexander, "Battery-utility interface using soft switched AC link supporting low voltage ride through", in *Proc. ECCE*, pp. 2606–2613, 2009.

[18] A. K. Balakrishnan, "Soft switched high frequency AC-link converter", M.S. thesis, Elect. Comput. Eng. Dept., Texas A&M Univ., College Station, TX, USA, 2008.